Electronic Supplementary Material (ESI) for Journal of Materials Chemistry A.
This journal is © The Royal Society of Chemistry 2017

SUPPORTING INFORMATION

Chiroptical, morphological and conducting properties of chiral nematic mesoporous cellulose / polypyrrole composite films

Erlantz Lizundia,[a,b] Thanh-Dinh Nguyen,[b] Jose L. Vilas,[a] Wadood Y. Hamad,[c] Mark J. MacLachlan*[b]*

[a]Macromolecular Chemistry Research Group (LABQUIMAC), Department of Physical Chemistry, Faculty of Science and Technology, University of the Basque Country (UPV/EHU), Leioa 48940, Spain.

[b]Department of Chemistry, University of British Columbia, 2036 Main Mall, Vancouver, BC, V6T 1Z1, Canada.

[c]FPInnovations, 2665 East Mall, Vancouver, BC, V6T 1Z4, Canada.

*E-mail: erlantz.liizundia@ehu.eus, mmaclach@chem.ubc.ca

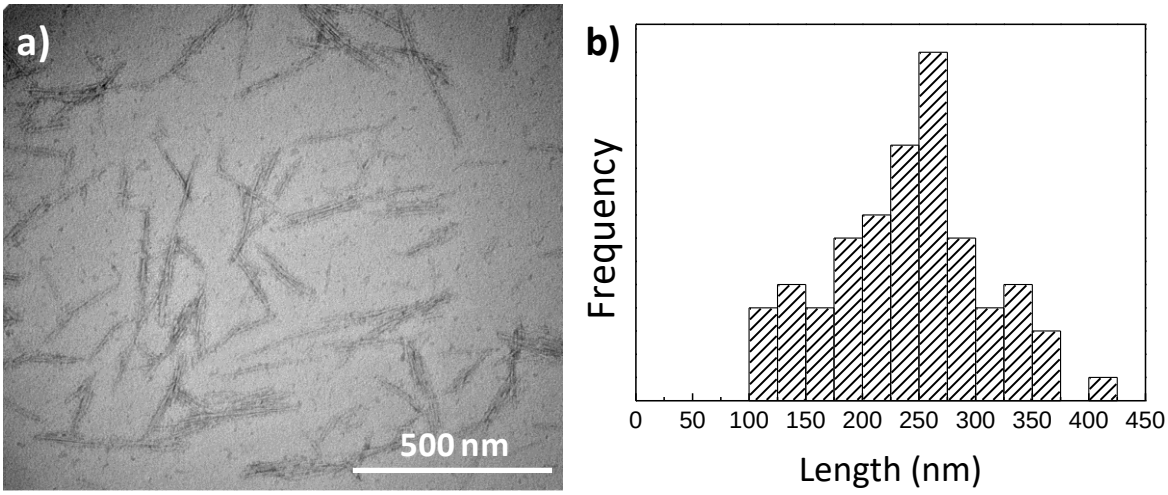

Fig. S1. a) Representative transmission electron microscopy (TEM) image and b) length distribution of CNCs (based on count of 90 particles).

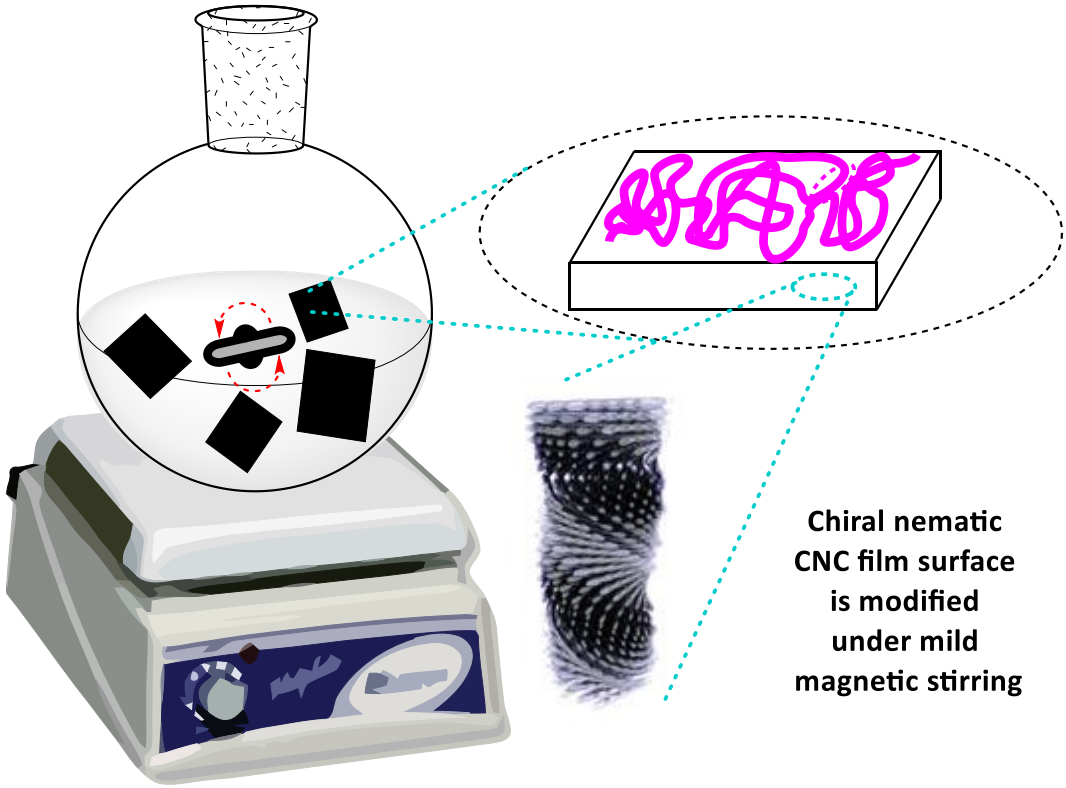

Fig. S2. Schematic representation showing the surface modification of chiral nematic CNC films. Pink lines represent the newly introduced moieties onto CNC films.

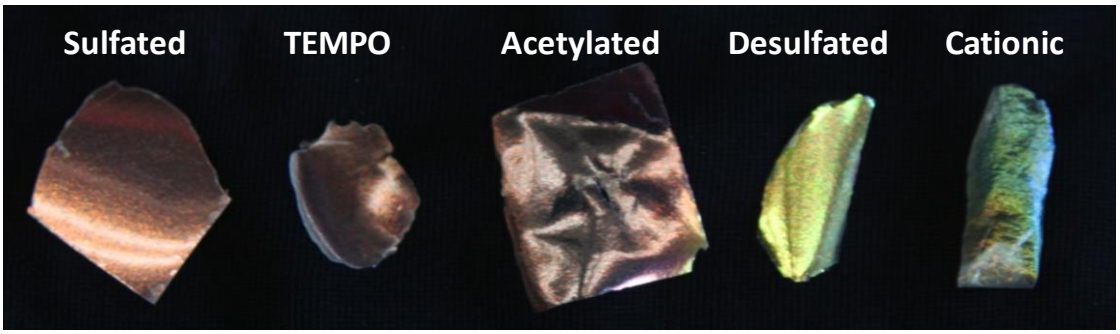

Fig. S3. Photograph of chiral nematic CNC films showing different iridescent properties upon surface modification.

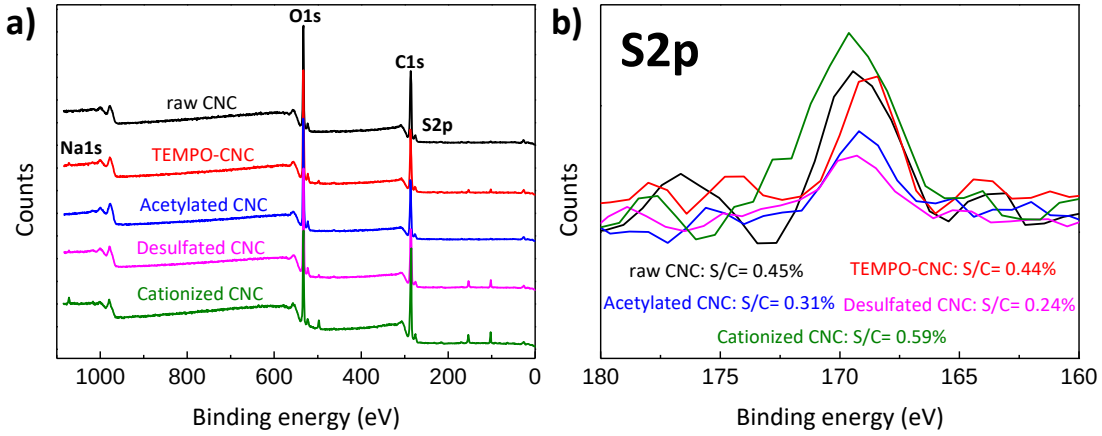

Fig. S4. a) XPS survey spectra and b) S2p sulfur spectra of modified films (S/C ratio is also shown).

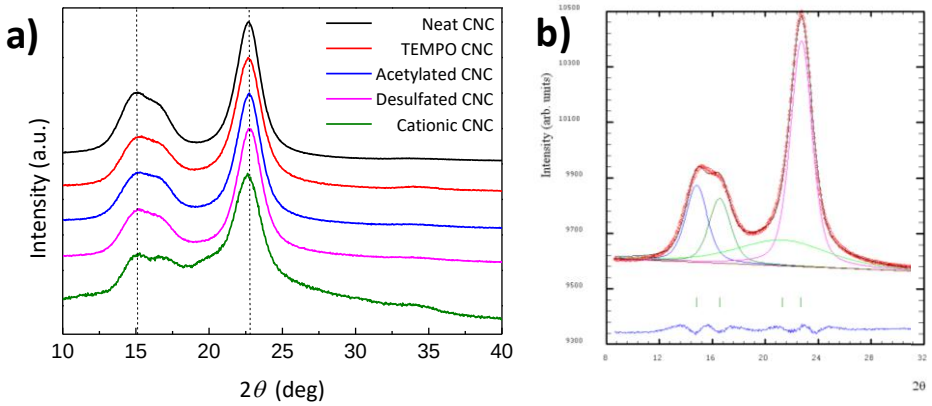

Fig. S5. a) PXRD patterns of surface-modified iridescent CNC films and b) diffraction pattern for acetylated CNC film resolved into crystalline peaks and amorphous background according to the Ruland–Rietveld analytical approach. The residual of the fit is shown at the bottom.

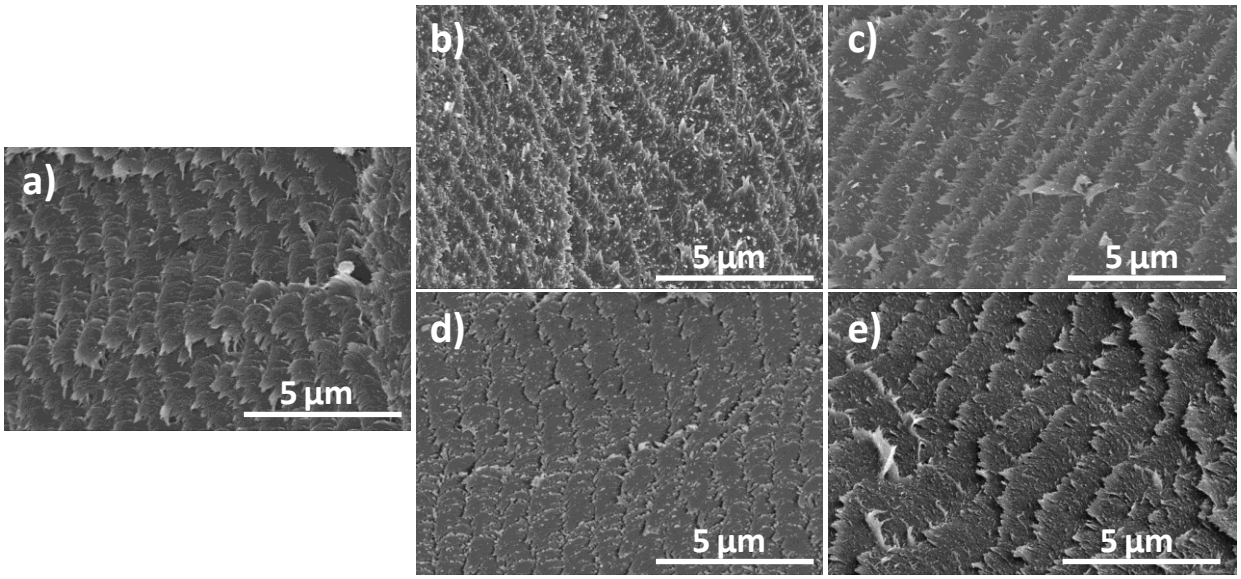

Fig. S6. FE-SEM micrographs viewed along fracture cross-sections of surface-modified CNC films showing the chiral nematic order of: a) sulfated; b) acetylated; c) TEMPO-oxidized; d) desulfated and e) cationic.

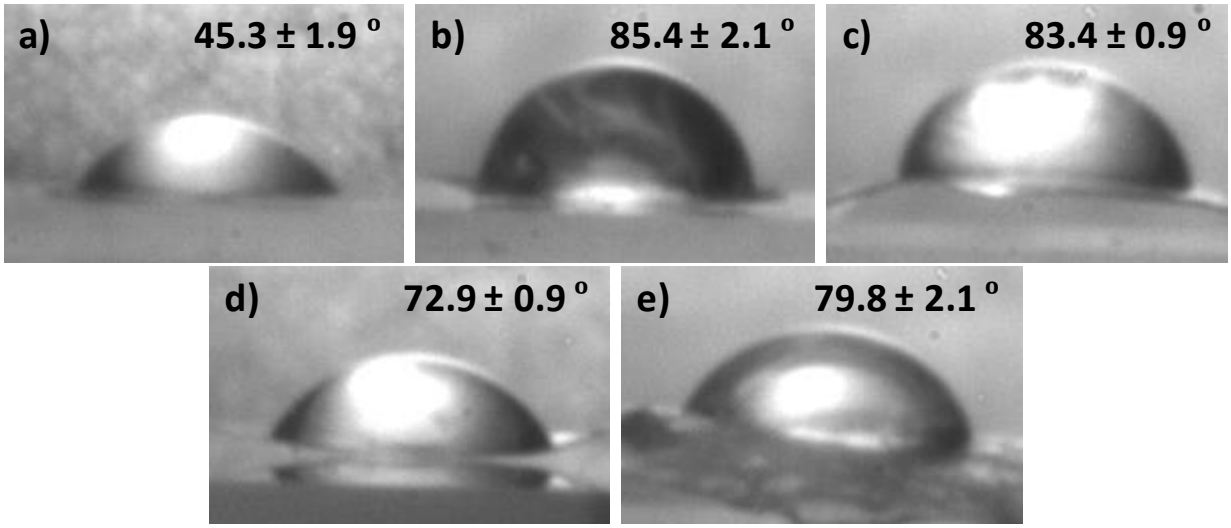

Fig. S7. Representative images of a water drop at the CNC surfaces (WCA values are highlighted). a) sulfated; b) TEMPO-oxidized; c) acetylated; d) desulfated and e) cationic CNC films.

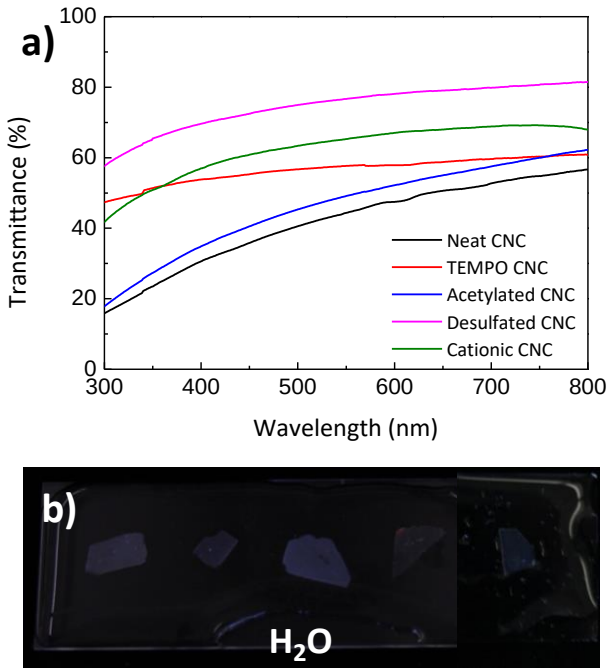

Fig. S8. Sensing performance of modified CNC films when soaked in water. a) UV-Vis spectra and b) the macroscopic appearance of the modified films.

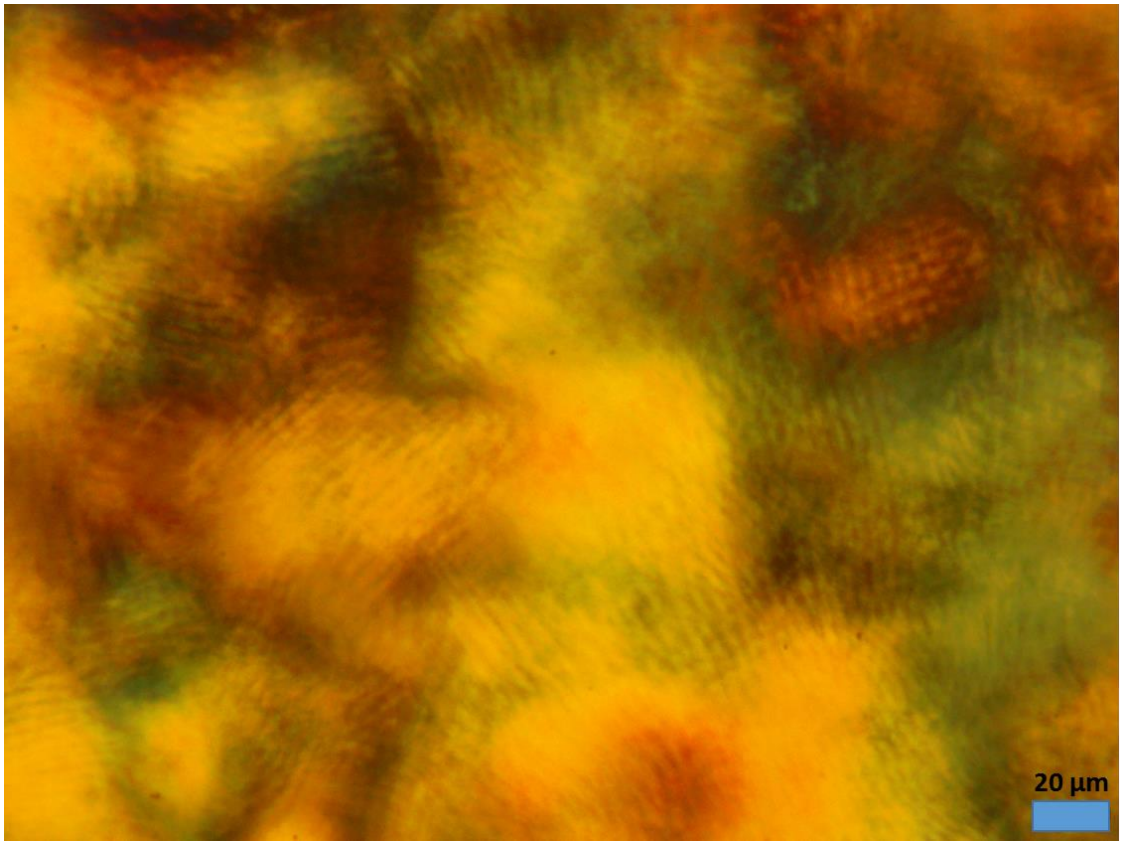

Fig. S9. Polarized optical microscopy image of a TEMPO-modified CNC film upon swelling in water. The POM images of this and the other samples showed similar textures when dried or swollen in ethanol or water.

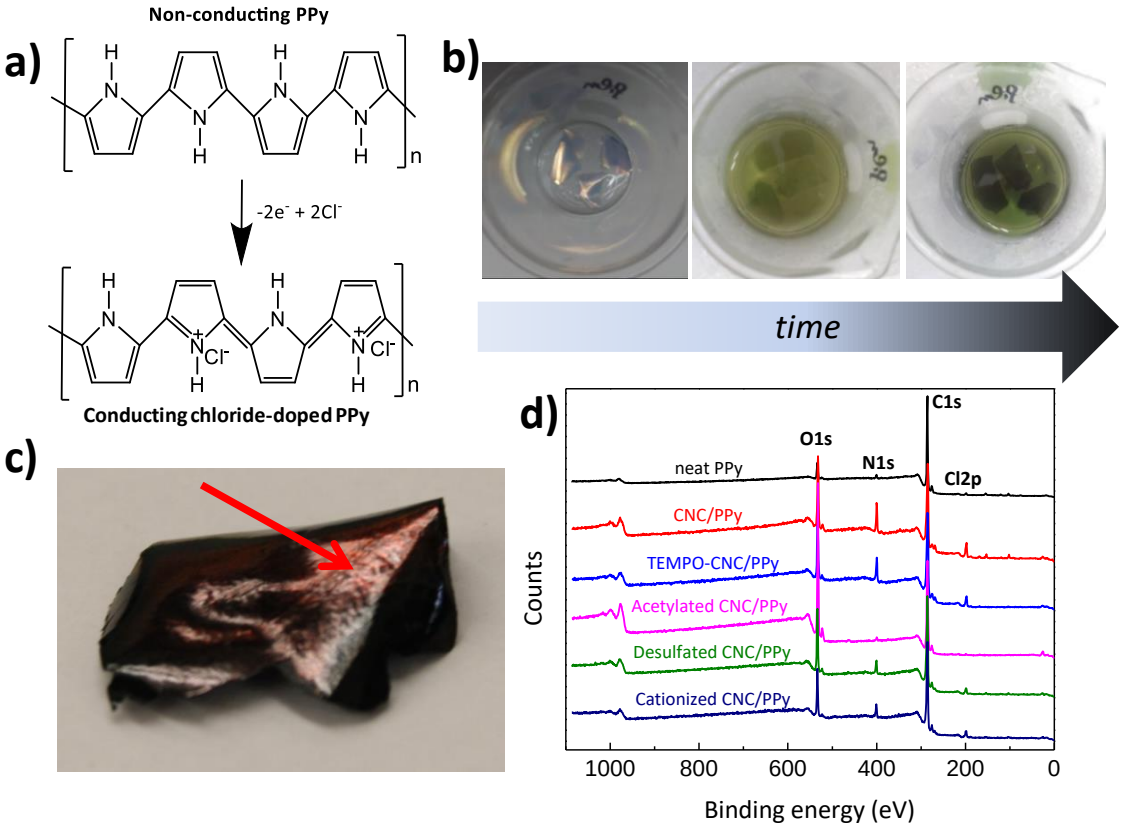

Fig. S10. a) Scheme showing both non-conducting (top, reduced) and conducting (bottom, oxidized) forms of polypyrrole; b) photographs acquired during PPy polymerization onto CNC surfaces showing a color change of the conductive films; c) photograph showing the iridescence of CNC/PPy films and d) XPS survey spectra of CNC/PPy composite films.

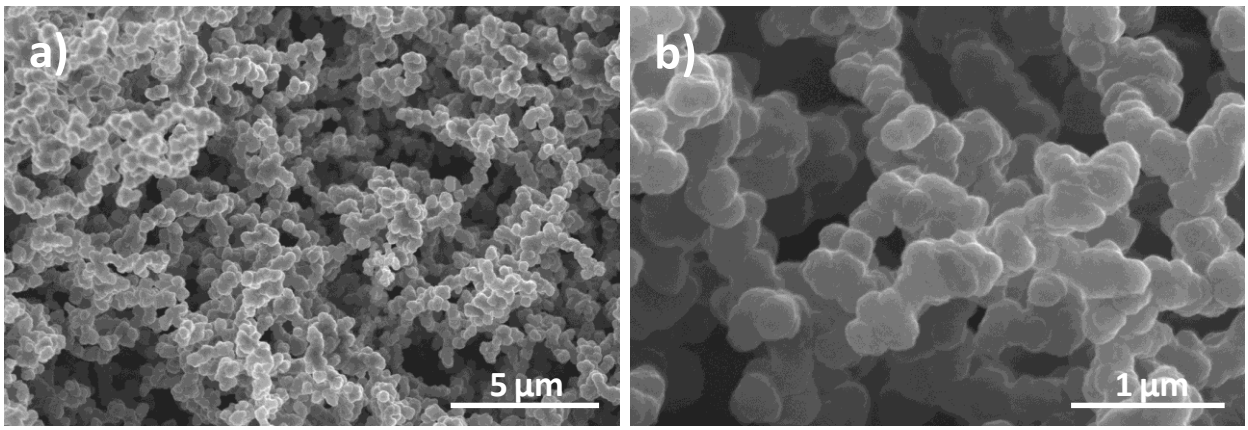

Fig. S11. SEM micrographs of the synthesized neat PPy at a) low and b) high magnification.

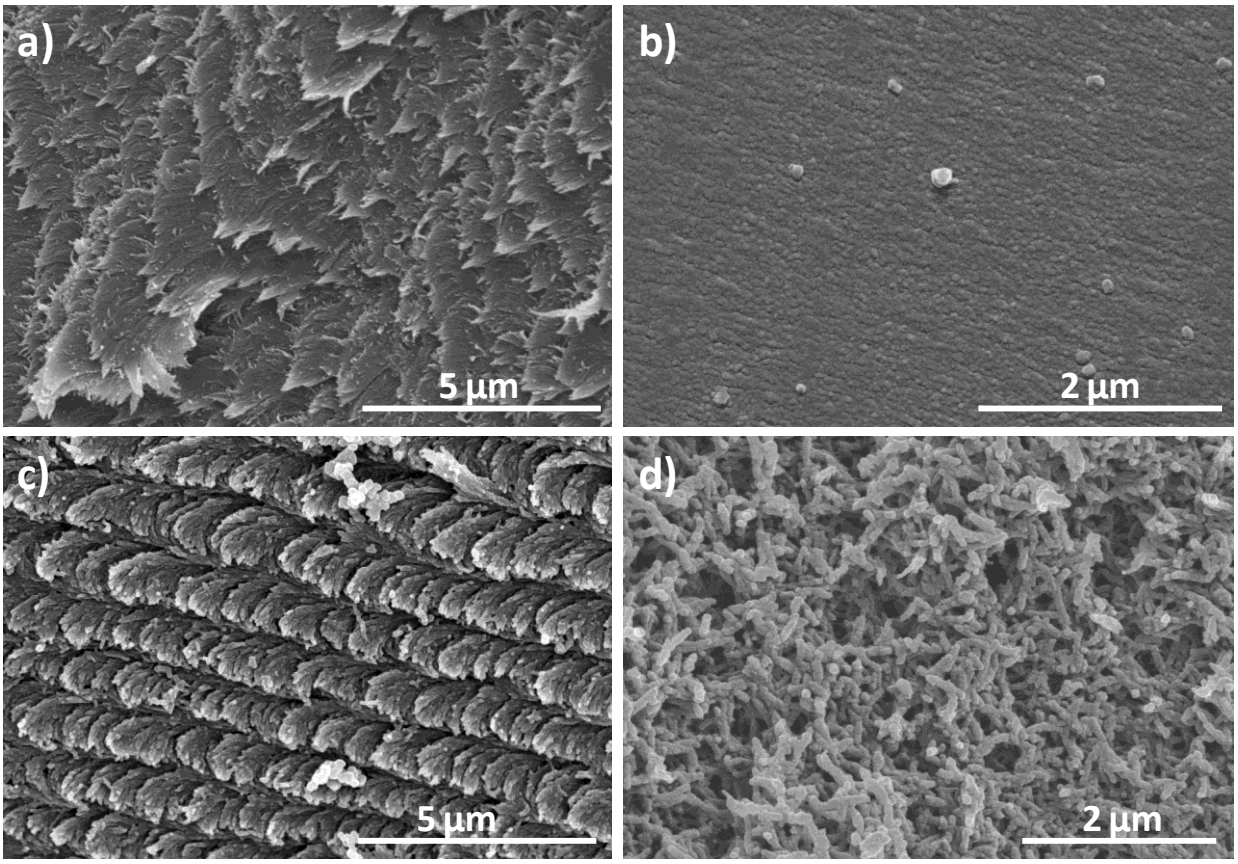

Fig. S12. SEM micrographs of the CNC/PPy composites having chiral nematic long-range organization. a) Edge view of CNC/PPy film; b) top view of the same film showing a flat PPy coating; c) edge view of TEMPO-oxidized CNC/PPy film and d) top view of the same film showing a rough PPy layer onto CNC film.

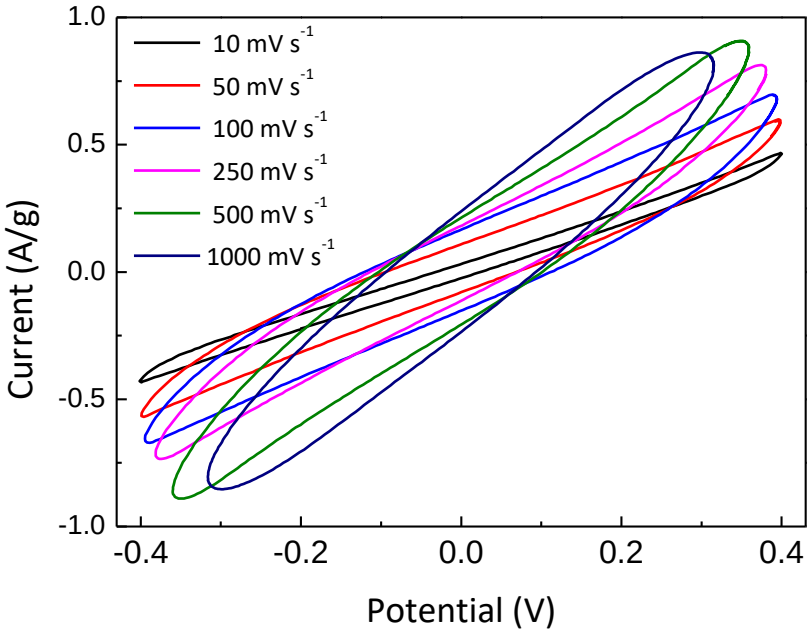

Fig. S13. Cyclic voltammograms of a CNC/PPy composite in 1 M KCl for scan rates varying from 10 to 1000 mV s^{-1}.

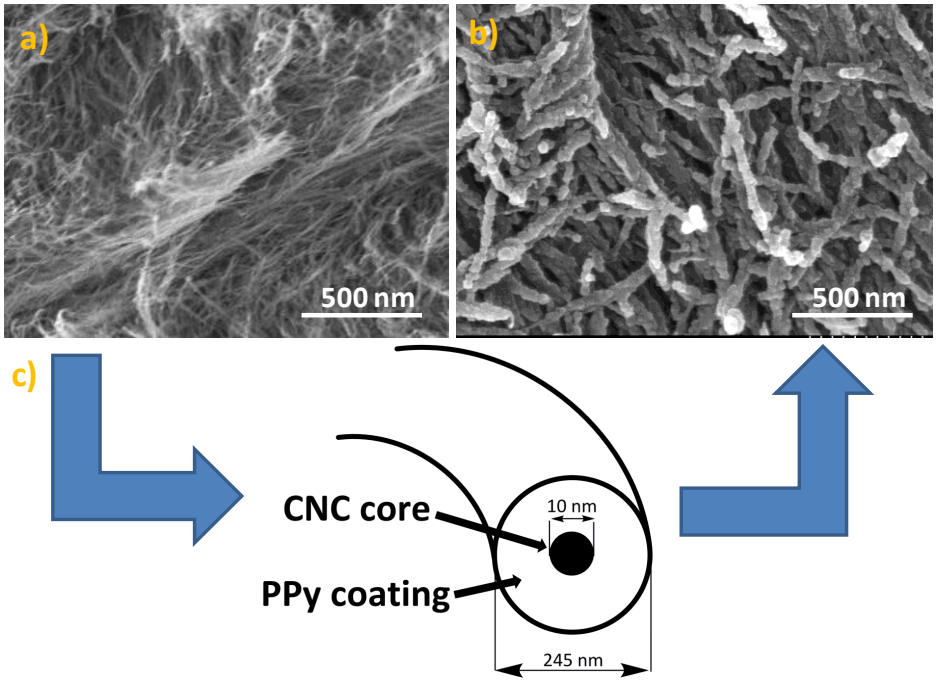

Fig. S14. FE-SEM images of a) CNMC-1 and b) CNMC/PPy-1. c) Schematic representation showing the PPy coating around CNCs until they are completely wrapped.

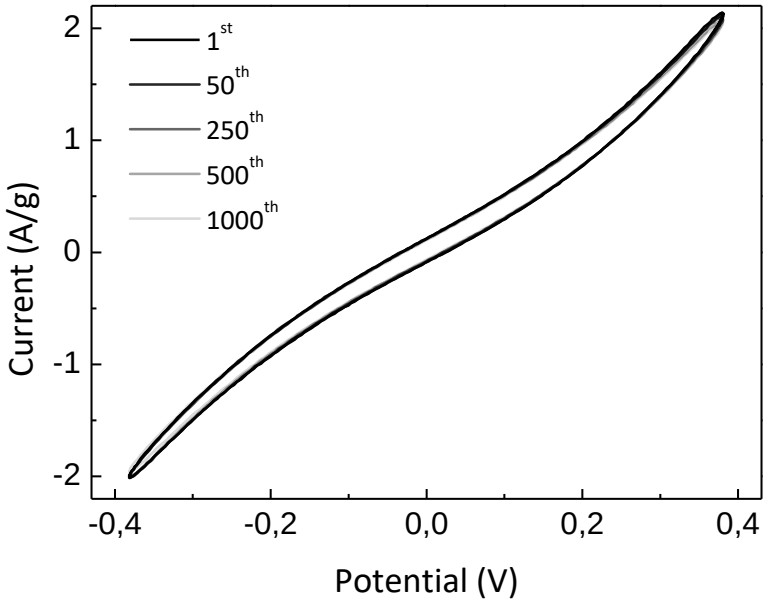

Fig. S15. Cycling performance of CNMC/PPy-3 at a scan rate of 250 mV s^{-1}.

Tables

Table S1. Crystallinity index (X_c) and *(200)* interplanar spacing values for modified CNC films.

Sample	X_c (%)	Interplanar spacing d_{200}
Native CNC	95	3.92 Å
TEMPO CNC	74	3.92 Å
Acetylated CNC	77	3.91 Å
Desulfated CNC	71	3.92 Å
Cationic CNC	62	3.93 Å

Table S2. XPS based surface atomic percentages for modified CNC films. Data between parentheses represent S mass content (%).

Sample	Atomic content (%)				O/C[a]
	C	O	S	Na	
Native CNC	68.89	30.80	0.31 (0.75)	-	0.45
TEMPO CNC	61.91	37.43	0.28 (0.66)	0.38	0.61
Acetylated CNC	60.10	39.74	0.20 (0.47)	-	0.66
Desulfated CNC	64.71	34.92	0.16 (0.38)	0.19	0.54
Cationic CNC	72.04	26.60	0.44 (1.08)	0.92	0.37

[a] The theoretical O/C ratio for cellulose is ~0.83. We don't have an explanation for the consistently low O/C ratio observed, but it may be due to the shallow penetration depth of the XPS technique.

Table S3. XPS based surface atomic percentages for CNC/PPy composite films. Data between parentheses represent S mass content (%).

Sample	Atomic content (%)					Cl/N
	C	O	S	N	Cl	
PPy	89.51	7.58	-	2.16	0.75	0.35
CNC/PPy	65.75	19.54	0.66 (1.52)	10.84	3.21	0.29
TEMPO CNC/PPy	72.25	15.99	0.19 (0.45)	9.15	2.42	0.26
Acetylated CNC/PPy	61.41	36.72	0.21 (0.50)	1.45	0.21	0.15
Desulfated CNC/PPy	73.91	18.88	-	5.57	1.64	0.29
Cationic CNC/PPy	78.29	14.14	-	5.44	2.13	0.39

References

1 T. D. Nguyen, K. E. Shopsowitz and M. J. MacLachlan, *J. Mater. Chem. A*, 2014, **2**, 5915–5921.